Electronic Supplementary Material (ESI) for Nanoscale.

Nanopatterned dual reactive surface-driven block copolymer self-assembly

Coste Mawélé Loudy [1,2], Joachim Allouche [1], Antoine Bousquet [1],
Hervé Martinez [1], Laurent Billon [1,2]**

[1] CNRS/Université de Pau et des Pays de l'Adour/E2S UPPA, IPREM CNRS-UMR 5254 Hélioparc, 2 avenue Président Angot, 64053 Pau Cedex 9, France

[2] Bio-inspired Materials Group: Functionality & Self-assembly, Université de Pau et des Pays de l'Adour, IPREM CNRS-UMR 5254, Hélioparc, 2 avenue Président Angot, 64053 Pau Cedex 9, France

Corresponding Authors:
Herve.martinez@univ-pau.fr
Laurent.billon@univ-pau.fr

SUPPORTING INFORMATIONS

Experimental section

Materials. Propargyl-PEG4-thiol (90%) was brought from Brodpharm (USA). The Blocbuilder® alkoxyamine and the nitroxide radical (SG1 solution) were obtained from ARKEMA. All other chemicals were purchased from Sigma Aldrich and used without further purification except copper bromide CuBr which was purified by stirring with acetic acid overnight, washing with acetic acid, absolute ethanol and diethyl ether before finally be dried in a vacuum oven.

Characterization.

^{1}H NMR experiments were carried out on a Bruker 400 MHz spectrometer in CDCl3 at 27 °C. All spectra were recorded on a Bruker AVANCE 400 MHz spectrometer. Chemical shifts are reported as ppm downfield from Tetramethyl silane TMS.

The molecular weight and dispersity of all synthesized polymers were measured using size exclusion chromatography SEC using THF as eluent (flow rate 1.0 mL min^{-1}) at 30 ^{o}C. SEC is equipped with a Viscotek VE 5200 automatic injector, a pre-column and two columns (Styragels HR 5E and 4E (7.8 ´ 300 mm)) and 4 detectors: UV-visible spectrophotometer (Viscotek VE 3210), a Multi-angle Light Scattering detector (Wyatt Heleos II), a viscosimeter (Wyatt Viscostar II) and a refractive index detector (Viscotek VE 3580). Polystyrene standards were used to determine the dispersity of the polymers.

UV-Vis spectroscopy measurements were carried out in spectrum mode using a SHIMADZU UV-2450 spectrophotometer controlled by a software. The sample was solubilized before analysis in an appropriate solvent and inserted in a quartz cell having an optical path length of 1 cm.

XPS measurements of most the samples were performed on a Thermo K-alpha spectrometer with a hemispherical analyzer and a microfocused (400 µm diameter microspot) monochromated radiation (Al Kα, 1486.6 eV) operating at 72 W under a residual pressure of 1.10^{-9} mbar. The pass energy was set to 20 eV. Charge effects, currently important for hybrid sample, were compensated by the use of a dual beam charge neutralization system (low energy electrons and Ar^{+} ions) which had the unique ability to provide consistent charge compensation. All spectra containing polystyrene or aromatic carbons were energy calibrated by using the aromatic double bond peak at a binding energy of 284.5 eV. When there was no aromatic carbons, the binding energy scale was calibrated from the hydrocarbon peak at 285 eV. Spectra

were mathematically fitted with Casa XPS software© using a least squares algorithm and a nonlinear Shirley-type background. The fitting peaks of the experimental curves were defined by a combination of Gaussian (70%) and Lorentzian (30%) distributions. Quantification was performed on the basis of Scofield's relative sensitivity factors. [1]

High resolution spectra of Nitrogen containing samples for both azide and triazole environments were performed using an Escalab 250 Xi spectrometer using a monochromatized Al Kα radiation (hν = 1486.6 eV). To avoid the degradation of nitrogen in both azide and triazole environments, liquid nitrogen was used to maintain the sample holder at -88 °C throughout the analysis. Charge compensation mode was also used, and core spectra were recorded using a 20 eV constant pass energy with a 0.15 eV step size and short time.

Atomic force microscopic AFM images were obtained using MultiMode® 8 Atomic Force Microscope from Bruker in a PeakForce Quantitative NanoMechanics QNM mode.

Transmission Electron Microscopy images of gold nanoparticles were performed on a Philips CM 200 (200 kV) TEM microscope equipped with a LaB6 source. The particles dispersed in Ethanol were dropped onto a carbon-coated copper grid and dried before analysis.

Contact Angle measurements were done using an instrument designed in the Lab. The apparatus was made of an optical bench equipped with a heat control unit that can reach till 200 °C, a humidity control system and an ethernet camera that can record 30 images per second. Angle angles were obtained through the analysis of the images using LabVIEW software.

Synthesis

Synthesis of polystyrene-block-poly(4-vinylbenzylazide) PS-b-PVBN$_3$.

PS-*b*-PVBN$_3$ block copolymer used in this work was synthesized using Nitroxide-Mediated Polymerization NMP and nucleophilic substitution (Scheme SI1). The NMP is based on a reversible termination mechanism of a growing chain by a nitroxide, leading to an activation-deactivation equilibrium between the predominant species (dormant chains) and a minority of growing propagating radicals. The dormant species are able to dissociate in a propagating radical (also called growing chain) and a persistent radical (also called nitroxide) through a homolytic rupture by an increase of the temperature. NMP can be used to generate block copolymer, the first polymer block bearing the nitroxide end-group acts as a macro-initiator to polymerize another monomer.

PS-*b*-PVBN$_3$ was synthesized in three steps as reported in Scheme SI1. In the first step, styrene (144 mmol), the Blocbuilder® alkoxyamine (0.2 mmol) and the nitroxide radical (SG1 solution, 0.03 mmol, 15%) were added to a round bottom flask of 50 mL. The flask was sealed with a septum, put in an ice bath, degazed for twenty minutes with nitrogen and immersed in an oil bath at 115 °C for 5h to reach 50 % of conversion (determined by ^{1}H NMR). The resulting viscous mixture of polystyrene PS and the remaining styrene was precipitated twice in methanol to remove the remaining monomer, filtered and dried at room temperature under vacuum. In the second step, 500 mg of the dried powder of PS (0.014 mmol) were dissolved in 5 mL of dimethylformamide DMF overnight. After solubilizing PS, the 50 mL round bottom flask was put in an ice bath. 4-vinylbenzylchloride VBC (11.4 mmol) and nitroxide radical (SG1 solution, 0.002 mmol, 15%) were added, the flask was sealed with a septum and the mixture was degazed for 20 minutes with nitrogen and immersed in an oil bath at 115 °C. After 1h, the reaction was stopped and the resulting block copolymer was precipitated twice in methanol, filtered, and dried at room temperature under vacuum. The resulting block copolymer PS-*b*-PVBC was analyzed analyzed by ^{1}H NMR and size exclusion chromatography SEC in THF to determine its composition. In the last step, the new block copolymer (PS_{330}-*b*-$PVBC_{150}$, 0.5g, 8.3×10^{-3} mmol), sodium azide (2.5 mmol) and DMF (10 mL) were put in a round bottom flask and mixed at room temperature for 3 days to allow the substitution of the chlorine atoms in PVBC block by the azide group. The salts were removed by Büchner filtration using a Whatman® membrane filter nylon of 0.8 µm pore size. After the filtration, the polymer solution was precipitated in methanol twice and dried at room temperature under vacuum. The final block polymer was analyzed by SEC in THF, ^{1}H NMR and XPS to confirm the replacement of the chlorine atoms by the azide groups and the determine the composition which was calculated to be PS_{330}-*b*-$(PVBN_3)_{150}$.

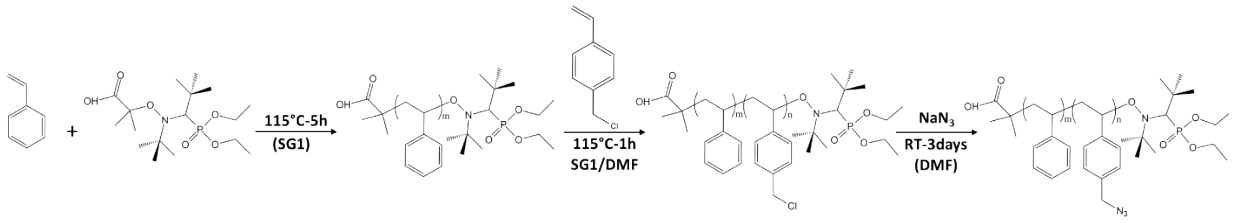

Scheme SI1. Synthetic way towards the formation of PS-*b*-PVBN$_3$.

Synthesis of ethynyl terminated poly(N-isopropylacrylamide) Ethynyl-PNIPAM. The elaboration of a hybrid functional surface from self-assembled films of PS-*b*-$PVBN_3$ studied in this work was done through a chemical grafting *via* Huisgen cycloaddition between azide groups at the surface of PS-*b*-$PVBN_3$ film, alkyne functionalized gold particles and alkyne functionalized PNIPAM. For this reason, propargyl-terminated PNIPAM was synthesized by ATRP using propargyl 2-bromoisobutyrate, an ATRP initiator with a carbon-carbon triple bond. PNIPAM being a thermosensitive polymer, many factors such as molar mass, nature of the solvent or the polymer chain ends can have an effect of the thermoresponsive behavior of the polymer, affecting thereof its controlled polymerization.[2–4] To avoid such impropriety, water-assisted ATRP of NIPAM was performed through a mixture of water and tert-butanol (1:4 v%) inspired from a synthesis reported by Ye and *al.*.[5] This procedure allows the synthesis of PNIPAM with high conversion and a narrow dispersity. Firstly, 5 mL of a mixture of tert-butanol and water (4:1) was degassed in a Schlenk flask sealed with a septum. The tube was frozen in liquid nitrogen and degassed via 3 consecutive freeze-pump cycles. Then 1 mL was taken out of the degassed 5 mL and mixed with the initiator (propargyl 2-bromoisobutyrtate, 18 mg) while N-isopropylacrylamide (NIPAM, 8.8 mmol) was added to the remaining 4 mL. The tube was stirred, frozen again in liquid nitrogen and degassed via 3 consecutive freeze-pump cycles, filled with nitrogen before quickly adding CuBr (12.7 mg) and PMDETA (15.3 mg). The tube was evacuated and backfilled with nitrogen three times, stirred and purged for 15 minutes before adding with a syringe the degassed 1 mL solution containing the initiator via the septum under a strong nitrogen flux to start the polymerization. The flask was kept in an ice bath for 4h. The experiment was stopped by opening the flask to expose the catalyst to air. The resulting mixture was filtered through an alumina column to remove copper and dialysis was used to remove free monomers and purify the ethynyl-PNIPAM. The mixture was diluted with ethanol and dialyzed with deionized water using a regenerated cellulose membrane RC (weight cut off: 2 kDa) for 4 days. Water was changed twice a day during the purification process. The polymer was recovered by lyophilization and characterized by ^{1}H NMR, SEC in THF and XPS.

Synthesis of Propargyl-PEG4-thiol-capped gold nanoparticles GNPs@propargyl. Small propargyl-PEG4-thiol-capped gold nanoparticles were prepared in one step. Propargyl-PEG4-thiol (propargyl) ligand and $HAuCl_4.6H_2O$ salt were solubilized in 20 mL of absolute ethanol at a concentration of 2.5 mM for both reagents. 0.6 mL of a 0.1M $NaBH_4$ solution was then

added at once in the gold solution under a constant and strong stirring. The solution turned from yellow to a wine-red color. The mixture was stirred for 30 minutes to complete the fixation of the thiol ligand on the surface of gold particles, stopped and dialyzed against deionized water using a regenerated cellulose membrane RC (weight cutoff: 3.5 kDa) for 3 days to remove salt and unbound propargyl-PEG4-thiol. For that, water was changed twice a day during the purification process. Finally, the membrane was dialyzed against ethanol to get a final suspension of propargyl-PEG4-thiol-capped gold nanoparticles in ethanol.

Films preparation. Films were prepared through a drop-casting process. A 10 $g.L^{-1}$ solution of PS-*b*-$PVBN_3$ in chloroform was carefully drop-casted on a microscope glass slide to form a continuous film after the evaporation of the solvent. This led to a well-organized structure with distinct domains of PS and $PVBN_3$ on which selective click reactions were performed were performed on the extreme surface of PS-*b*-$PVBN_3$, allowing therefore to chemically bind successively both inorganic nanoparticles with physical properties and an organic polymer with a thermosensitive behaviour. Propargyl-PEG4-thiol-capped gold nanoparticles were first clicked on $PVBN_3$ nanodomains. CuBr (4 mg), sodium ascorbate (4 mg) and PMDETA (5 µL) were added to a plastic tube containing 10 mL of ethanol with gold nanoparticles at 50 $mg.L^{-1}$. Finally, the microscope slide containing the self-assembled film was dipped into the mixture for overnight. Then the glass was vigorously washed in ethanol several times and whether dried before the click reaction with Ethynyl terminated PNIPAM using the same procedure.

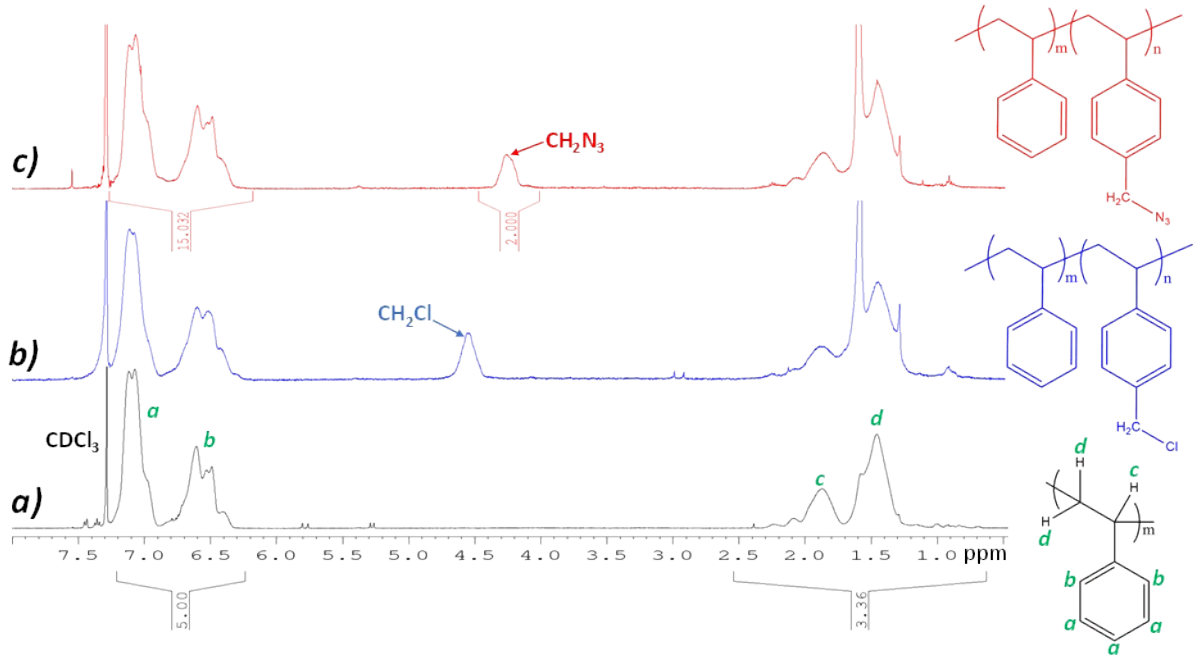

Figure SI1. (a) NMR spectrum of PS macro-initiator. (b) NMR spectrum of PS-*b*-PVBC. (c) PS-*b*-$PVBN_3$ final block copolymer after the substitution of chlorine groups by S_N2 reaction with azide groups.

^{1}H NMR analysis of PS macroinitiator and both copolymers, PS-*b*-PVBC and PS-*b*-$PVBN_3$ have been carried out to follow the chemical evolution of the products (Figure SI1). The complete shift of the signal from δ = 4.54 ppm, pertaining to the CH_2 bearing the chlorine atoms, to δ = 4.24 ppm, shows the success S_N2 reaction between the alkyl halide from PVBC and sodium azide NaN_3 in an aprotic solvent DMF. Using both, the area under of the peak at 4.24 ppm and the one of peaks in the region 6.3-7.2, we were able to discriminate the contribution of the aromatic protons from PS and the ones from $PVBN_3$. This allowed us to determine the molar composition of the final block copolymer. PS block had a DP_n equal to 330 (Table SI1) and the molar composition of the block copolymer calculated was PS_{330}-*b*-$(PVBN_3)_{150}$.

Table SI1. Summary of the polymers' characteristics.

Polymer	M_n [a] (g.mol^{-1})	DP_n [a]	M_n [b] (g.mol^{-1})	$Đ$ [b]	f^C PS
PS-BlocBuilder	35 000	330	32 000	1.1	1
PS-*b*- PVBN$_3$	57 000	330-150	49 000	1.2	0.63
Propargyl-PEG4-thiol *NP ligand*	--	--	248.3	--	--
Propargyl-PNIPAM	3 500	30	2 500	1.2	--

[a] calculated by ^{1}H NMR [b] Calculated from SEC with PS standards. [c] The volume fraction of PVBN$_3$ was calculated by using M_n calculated from ^{1}H NMR and the density of each polymer: ρ_{PS} = 1.05 g/mL and ρ_{PVBN3} = 1.14 g/mL. The density of PVBN$_3$ was calculated from the value of its Parachor (Sugden model[6]) using the following formula: $V = \frac{P}{2.596} + 2.966$ *where P is the Parachor and V the molar volume[7].*

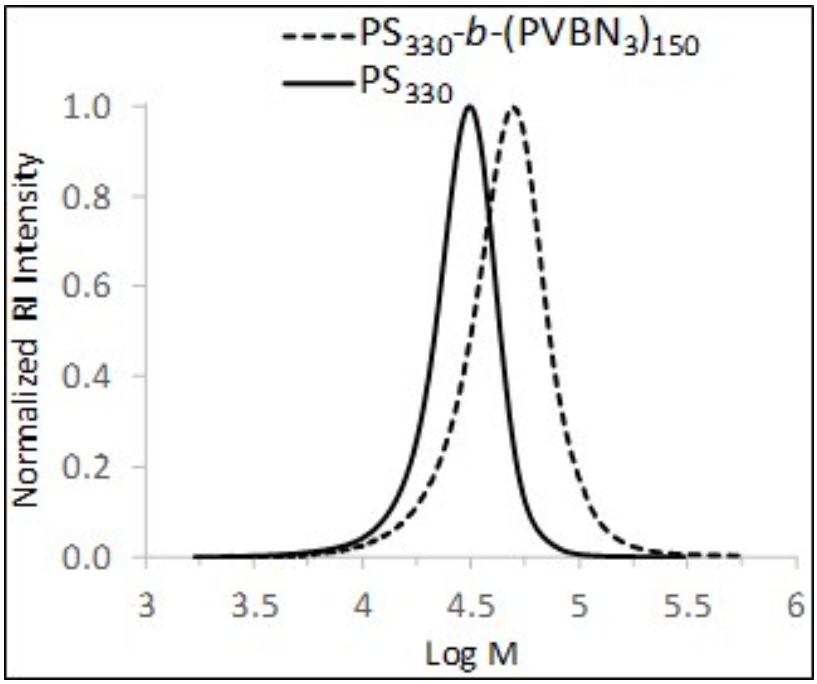

Figure SI2. SEC traces of the PS macro-initiator and PS-*b*-PVBN$_3$

The size exclusion chromatograms of both the macro-initiator PS-SG1 and the final block copolymer PS-*b*-PVBN$_3$ in THF are reported in supporting information (Figure SI2). A narrow dispersity was observed for PS ($Đ$ = 1.1) and PS-*b*-PVBN$_3$ ($Đ$ = 1.2) as reported in

literature for PS and derivatives synthesized by Nitroxide-Mediated Polymerization.[8,9] The molar mass of PS macro-initiator calculated from SEC analysis using PS calibration was equal to 32 000 g.mol^{-1}. The PS-*b*-PVBN$_3$ chromatogram showed a shift of the molar mass compared to the macro-initiator PS, proving an increase of the molar mass. The molar mass of PS-*b*-PVBN$_3$ calculated from SEC analysis using PS calibration was found to be equal to 49 000 g.mol^{-1}.

Propargyl terminated poly(N-isopropylacrylamide) Ethynyl-PNIPAM. The ^{1}H NMR spectrum of ethynyl-PNIPAM is depicted in Figure SI3a. All the characteristic peaks of PNIPAM can be observed. The peak of small intensity δ = 5.3 ppm belongs to the two protons in alpha position of the oxygen from the initiator. When the area under that peak was calibrated at 2 protons, the area under the peak at δ = 4 ppm was found to be 30, the degree of polymerisation of the polymer. This value allowed us to estimate the molar mass of the ethynyl-PNIPAM around 3500 g.mol^{-1}. The polymer was also analysed in size exclusion chromatography using THF as eluant (Figure SI3b). The molar mass calculated from SEC analysis using polystyrene calibration was 2500 g.mol^{-1}, giving sense to the value of the molar mass obtained by NMR.

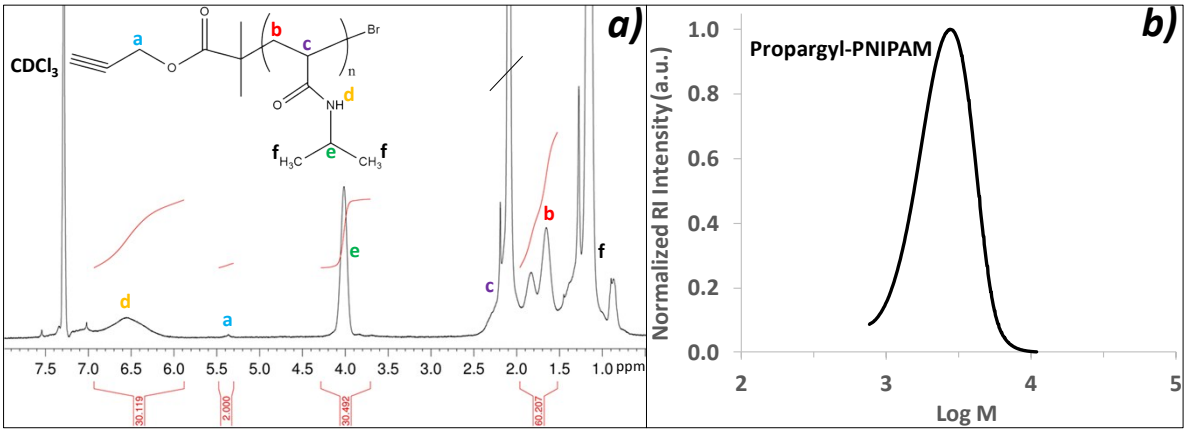

Figure SI3. (a) NMR spectrum and (b) SEC chromatogram of propargyl-PNIPAM.

For a better understanding and interpretation of experiments carried out with propargyl-PNIPAM, pure sample of the polymer was first analysed by XPS to serve as a reference before being grafted to PBVN$_3$ nanodomains. The C 1s, N 1s and O 1s high resolution spectra of

PNIPAM were deconvoluted as reported Figure SI4, with XPS quantification in agreement with the theoretical atomic composition of PNIPAM (Table SI2).

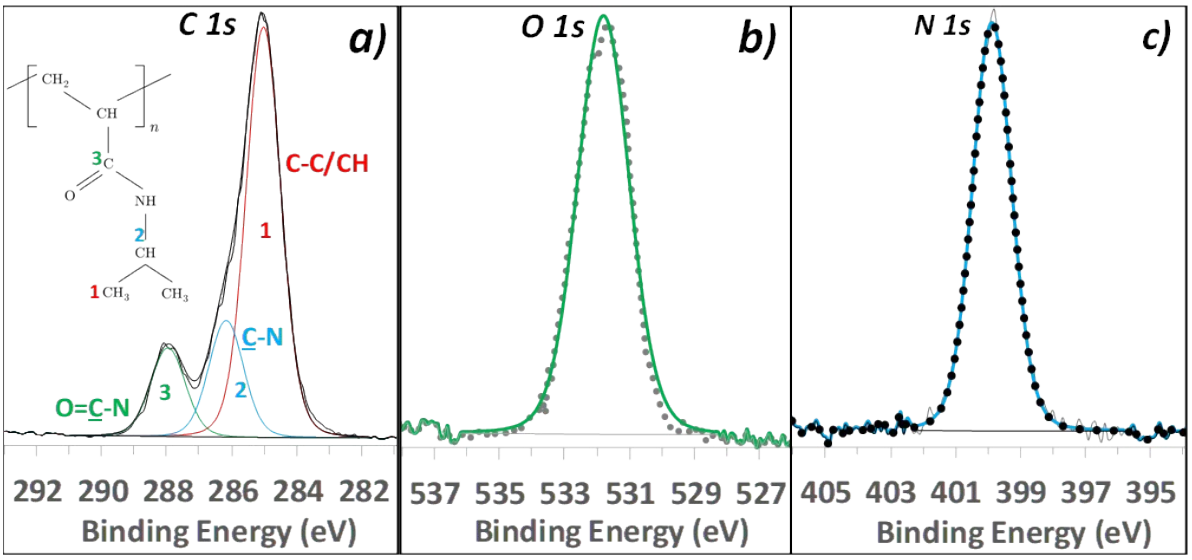

Figure SI4. C 1s (a), O 1s (b) and N 1s (c) high resolution spectra of propargyl-PNIPAM.

Table SI2. Atomic composition of propargyl-PNIPAM

Orbitals	Components	BE (eV)	FWHM (eV)	At. Conc. (%)	Theory (%)
	C−C/C−H	285.0	1.2	51.1	50
C 1s	C−N	286.2	1.2	14.4	12.5
	C=O	287.9	1.2	11.2	12.5
N 1s	N−C	399.9	1.4	9.6	12.5
O 1s	O=C	531.8	1.8	13.7	12.5

Propargyl-PEG4-thiol-capped gold nanoparticles GNPs@propargyl.

GNPs@propargyl were analysed by UV-Visible spectroscopy, Transmission Electron Microscopy and X-ray Photoelectron Spectroscopy. UV-Visible spectrum of the synthesized particles showed a maximum absorbance at 507 nm (Figure SI5a). The TEM micrograph, shown in Figure SI5b, exhibits spherical nanoparticles with an average diameter around 4 nm without any aggregation indicating their efficient stabilization by propargyl-PEG4-thiol ligand.

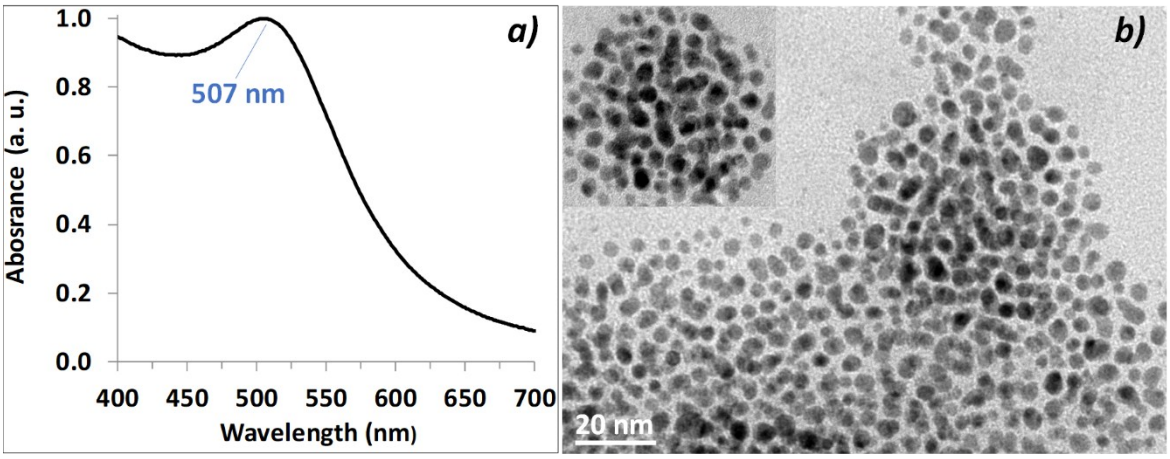

Figure SI5. (a) UV-vis spectrum and (b) TEM image of propargyl-PEG4-thiol-capped gold nanoparticles.

The attachment of the ligand on gold nanoparticles was further studied by XPS. Figure SI6 shows the high-resolution spectra of Au4f (from 81 to 93 eV) and S2p (from 157 to 169 eV). The former shows a double-component at 84.1 and 87.8 eV corresponding to Au $4f_{7/2}$ and Au $4f_{5/2}$ respectively, a typical proof of the presence of Au^0 state. Other components of small intensity are observed at higher binding energy, at 85.1 and 86.9 eV (for $Au^{1+}4f_{7/2}$ and $Au^{3+}4f_{7/2}$) and 88.6 and 89.9 eV (for $Au^{1+}4f_{5/2}$ and $Au^{3+}4f_{5/2}$), meaning that the oxidized state of Au is also present. As far as their atomic percentage contribution is concerned (Table SI3), it-s obvious that Au^0 refers to bulk nanoparticles (6.7 %) while the oxidized Au environments (1.7 %) are related to the surface modification generated through the binding process of sulphur onto gold nanoparticles[10,11]. This result is confirmed by the high resolution S2p core peak located at 163.4 ($2p_{1/2}$) and 162.2 eV $2p_{3/2}$) of a lightly reduced sulphur at the surface of gold nanoparticles. The binding energy of this peak is characteristic of reduced sulphur atoms, typically to the oxidation state -1 [12–14]. The C 1s and the O 1s spectra are also reported in Figure SI7. Four components can clearly be observed: C−C/C−H bonds from the aliphatic carbon at 285 eV, C-S/C−O bonds from propargyl-PEG4-thiol at 286.3 eV, C=O and COO bonds at 287.7 and 289.2 eV, probably from impurities of the commercial ligand (Figure SI8).

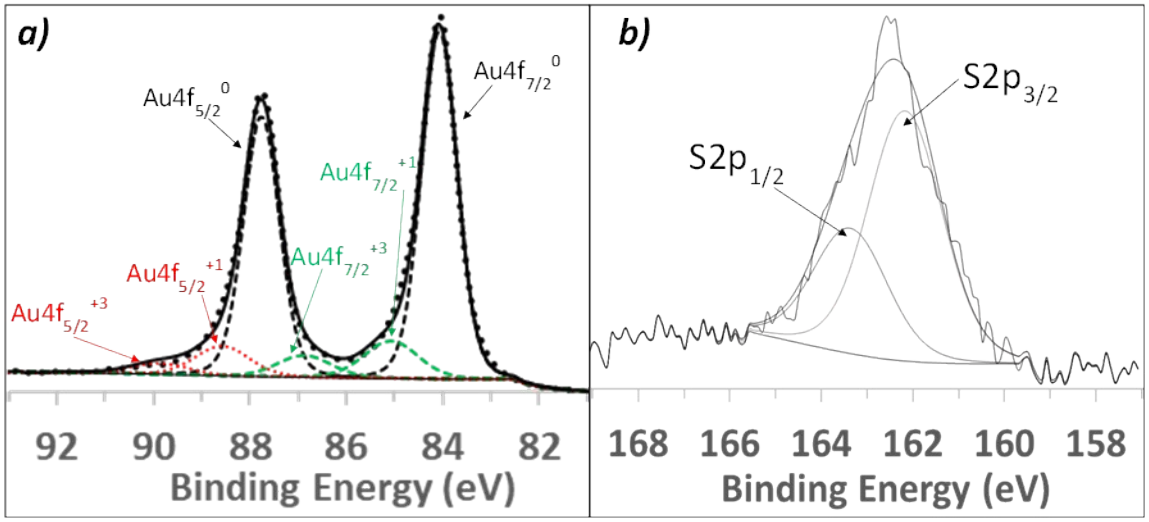

Figure SI6. (a) Peak fit of Au 4f from GNPs@propargyl-PEG4-thiol. (b) XPS spectrum of S 2p from Au-S bond. The fixation of Sulphur on Au surface displays a shift towards lower binding energy.

Table SI3. XPS data of GNPs@propargyl-PEG4-thiol analysed by XPS

Orbitals		Components	BE (eV)	FWHM (eV)	At. Conc. (%)
Au4f	Au°	$Au4f_{7/2-5/2}$	84.1−87.8	0.9−0.9	6.7
	Au_{ox}	$Au^{1+}4f_{7/2-5/2}$	85.1−88.6	1.3−1.3	1.7
		$Au^{3+}4f_{7/2-5/2}$	86.9−89.9	1.3−1.3	
S2p		$S2p_{3/2-1/2}$	162.2−163.4	2.0−2.0	4.4
C1s		C−C/C−H	285.0	1.3−1.3	26.7
		C−O/C−S	286.3	1.3−1.3	30.7
		C=O/O−C=O	287.7−289.2	1.7−1.7	9.2
O1s		O=C/O−C=O	532.1−534.1	1.6−1.2	7.6
		O−C	533.0	1.2	13.3

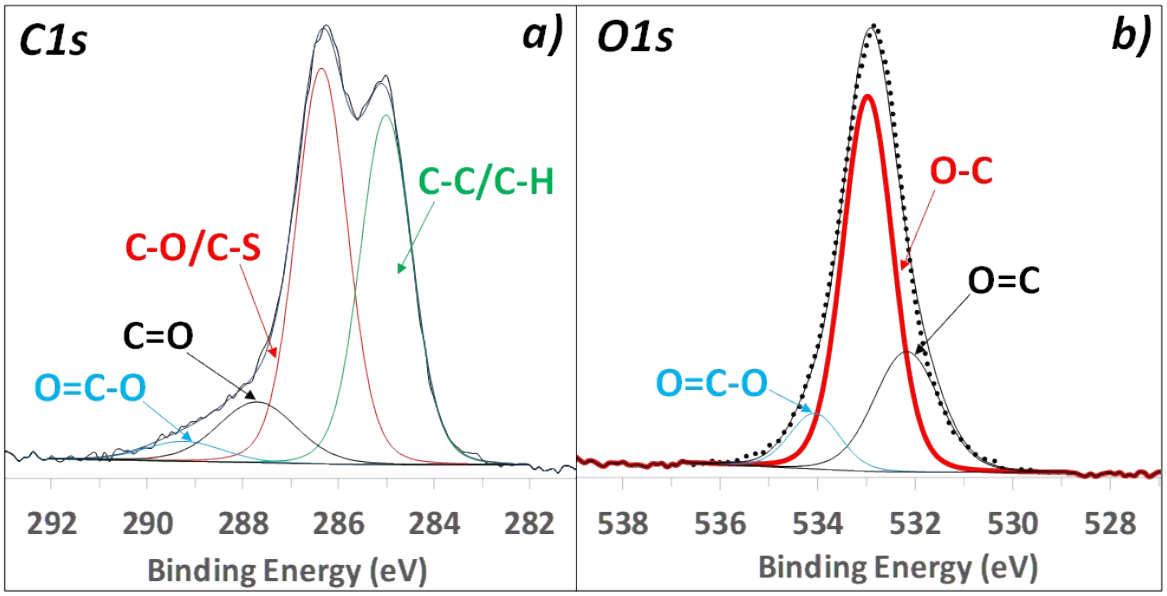

Figure SI7. C 1s (a) and O 1s (b) peak fits of GNPs@propargyl-PEG4-thiol.

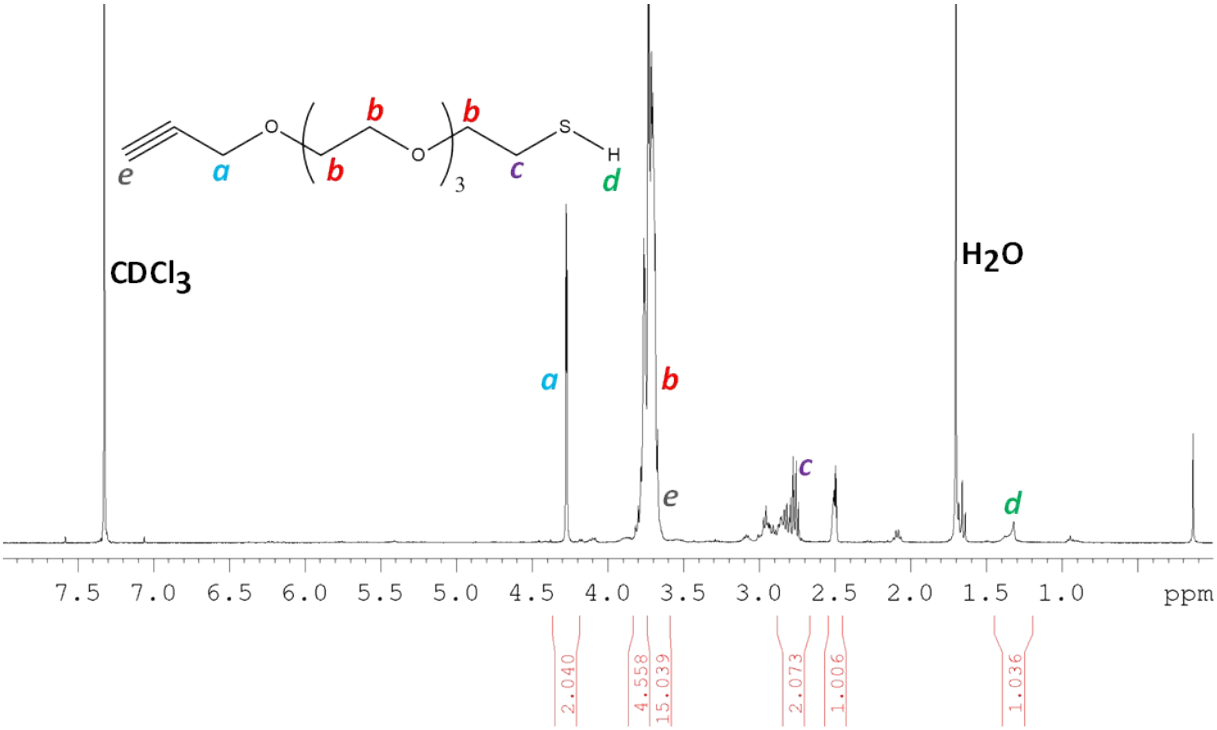

Figure SI8. ^{1}H NMR of propargyl-PEG-thiol in $CDCl_3$.

Table SI4. XPS data of PS-*b*-PVBN$_3$ film.

Orbitals	Components	BE (eV)	FWHM (eV)	At. Conc. (%)
C 1s	C=C (cycle)	284.5	0.9	65.2
	C−C/C−H	285.0	0.9	22.9
	C−N/C−O	286.2	1.1	2.4
	π-π*	290.5−292.2	1.3	7.2
N 1s	N^-/N−R	400.5	1.1	1.2
	N^+	404.3	1.1	0.6
O 1s	O 1s	532.3	1.4	0.5

Table SI5. XPS data of PS-*b*-PVBN$_3$ film grafted with GNPs@propargyl-PEG4-thiol

Orbitals	Components	BE (eV)	FWHM (eV)	At. Conc. (%)	
Au 4f	$4f_{7/2-5/2}$	84.2−87.8	1.4	0.25	
C 1s	C=C(cycle)	284.5	0.9	61.7	
	C−C/C−H	285.0	0.9	23.55	
	C−N/C−O/C−S	286.2	1.1	4.1	
	π-π*	291.3	1.6	5.7	
N 1s	N^-/N−R	400.5	1.1	1.0	1.9
	N2	401.0	1.3	0.25	
	N1	402.5	1.1	0.15	
	N^+	404.2	1.1	0.50	
O 1s	O−C	533.4	1.6	2.5	
S 2p	$2p_{3/2-1/2}$	162.4−163.6	1.7−1.7	0.3	

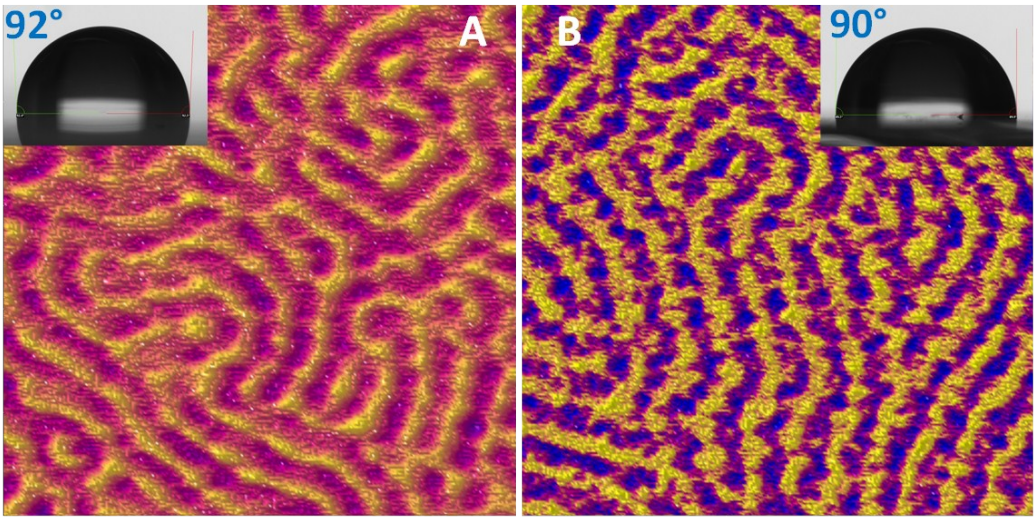

Figure SI9. AFM images (LogModulus mode) and Water contact angles of PS-*b*-PVBN$_3$ film (a) and PS-*b*-PVBN$_3$ grafted with GNPs@propargyl-PEG4-thiol (b).

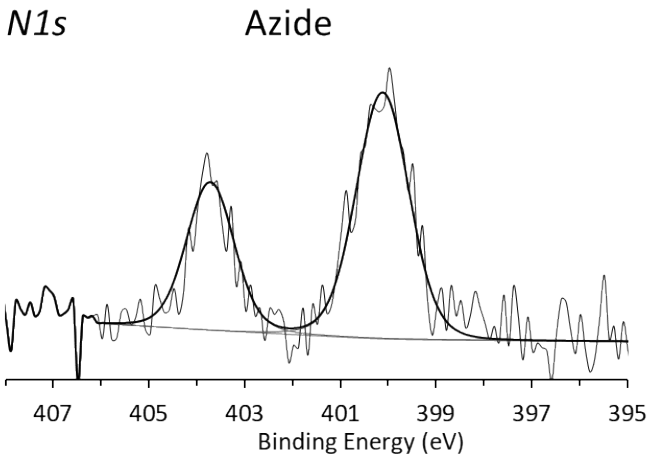

Figure SI10. XPS N1s spectrum of a control experiment made by reacting Ethynyl-PNIPAM on a PS-*b*-PVNN$_3$ film without the cycloaddition catalyst CuBr.

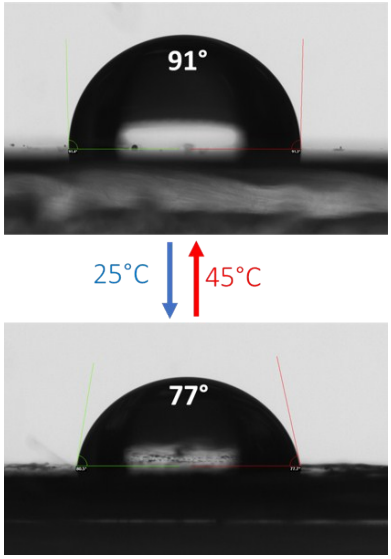

Figure SI11. Reversible wettability of PS-*b*-PVNN$_3$ film grafted with PNIPAM only

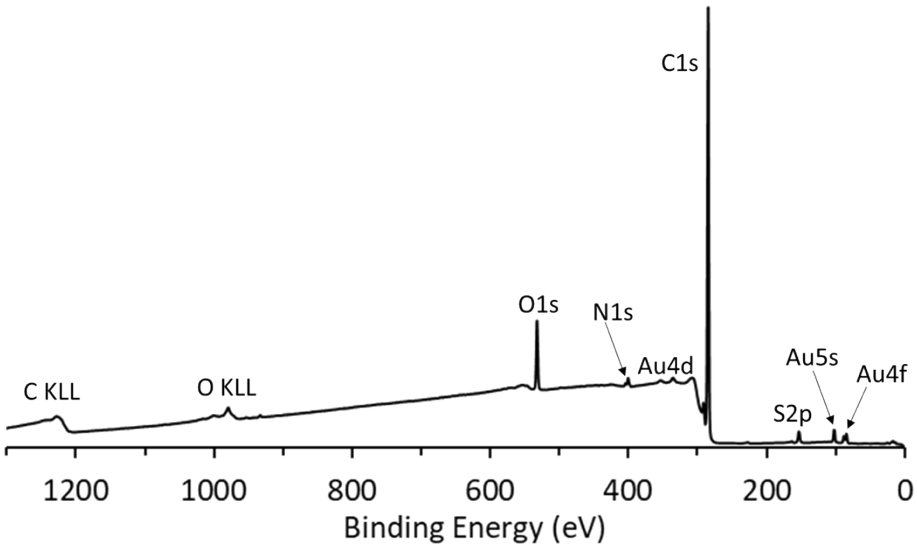

Figure SI12. XPS survey of PS-*b*-PVNN$_3$ film grafted with gold nanoparticles and PNIPAM, no impurities coming from reagent are detected.

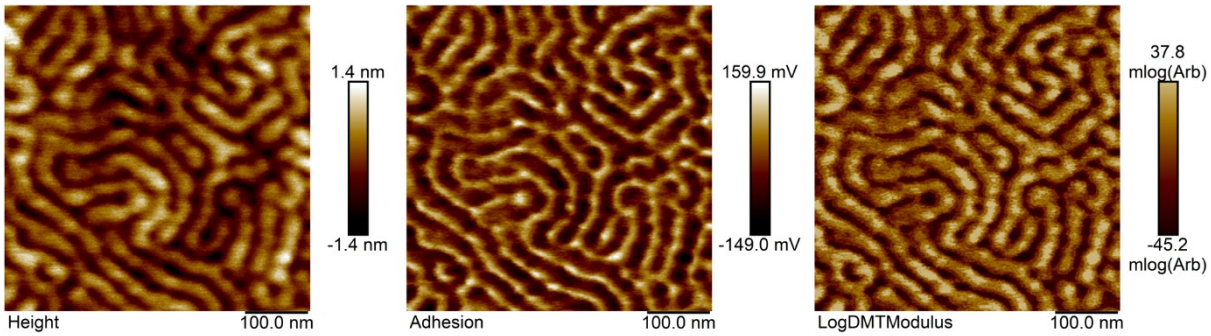

Figure SI13. AFM images of PS-*b*-PVBN$_3$ film.

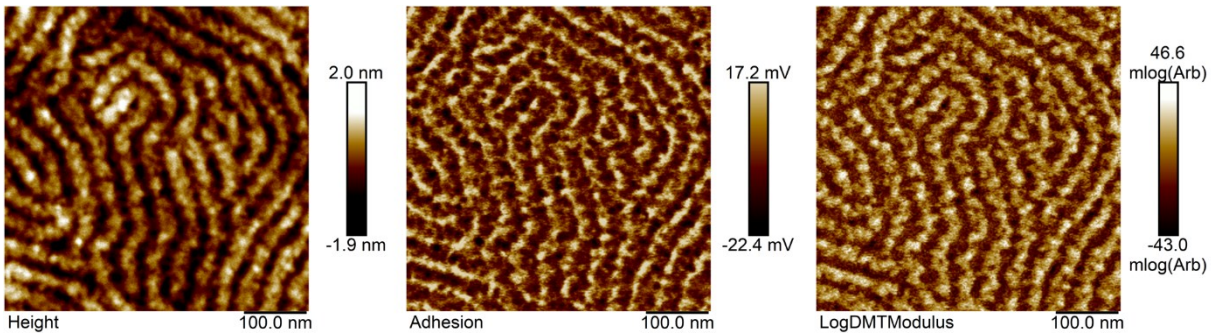

Figure SI14. AFM images of PS-*b*-PVBN$_3$ film grafted with GNPs.

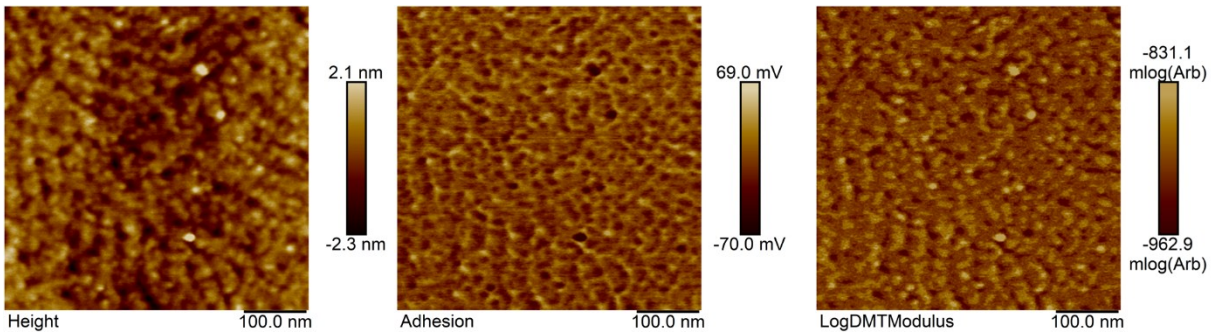

Figure SI15. AFM images of PS-*b*-$PVBN_3$ film grafted with PNIPAM.

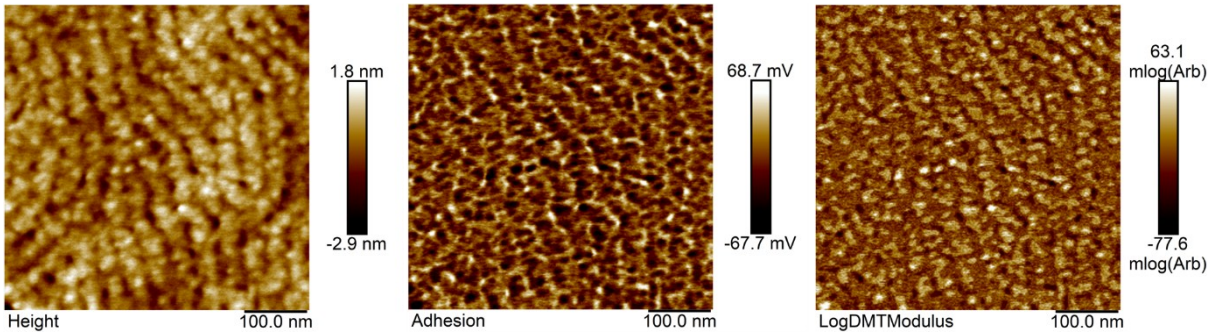

Figure SI16. AFM images of PS-*b*-$PVBN_3$ film grafted with both GNP and PNIPAM.

References:
1 J. H. Scofield, *J. Electron Spectrosc. Relat. Phenom.*, 1976, **8**, 129–137.
2 Y. Xia, X. Yin, N. A. D. Burke and H. D. H. Stöver, *Macromolecules*, 2005, **38**, 5937–5943.
3 H. Bouchékif and R. Narain, *J. Phys. Chem. B*, 2007, **111**, 11120–11126.
4 G. Masci, D. Bontempo, N. Tiso, M. Diociaiuti, L. Mannina, D. Capitani and V. Crescenzi, *Macromolecules*, 2004, **37**, 4464–4473.
5 J. Ye and R. Narain, *J. Phys. Chem. B*, 2009, **113**, 676–681.
6 S. Sugden, *J. Chem. Soc. Trans.*, 1924, **125**, 1177–1189.
7 J. H. Sewell, *J. Appl. Polym. Sci.*, 1973, **17**, 1741–1747.
8 R. B. Grubbs, *Polym. Rev.*, 2011, **51**, 104–137.
9 P. Marcasuzaa, S. Pearson, K. Bosson, L. Pessoni, J.-C. Dupin and L. Billon, *Chem. Commun.*, 2018, **54**, 13068–13071.
10 J. H. Johnston and K. A. Lucas, *Gold Bull.*, 2011, **44**, 85–89.
11 J.-P. Sylvestre, A. V. Kabashin, E. Sacher, M. Meunier and J. H. T. Luong, eds. P. R. Herman, J. Fieret, A. Pique, T. Okada, F. G. Bachmann, W. Hoving, K. Washio, X. Xu, J. J. Dubowski, D. B. Geohegan and F. Traeger, San Jose, Ca, 2004, p. 84.
12 P. Jiang, S. Xie, J. Yao, S. He, H. Zhang, D. Shi, S. Pang and H. Gao, *Chin. Sci. Bull.*, 2001, **46**, 996–998.
13 H. Guesmi, N. B. Luque, E. Santos and F. Tielens, *Chem. - Eur. J.*, 2017, **23**, 1402–1408.
14 S. Roux, B. Garcia, J.-L. Bridot, M. Salomé, C. Marquette, L. Lemelle, P. Gillet, L. Blum, P. Perriat and O. Tillement, *Langmuir*, 2005, **21**, 2526–2536.